Discover Applied Sciences

Research

Effects of factors from practical workpieces on ultrasonic LCR method stress measurement

Hsuan-Han Lai[1] · Deng-Han Yan[1] · Wei-Jheng Chang[2] · Kun-Hsien Chung[2] · Li-Xue Xing[2] · Wei-Ting Chang[2] · Weite Wu[1]

© The Author(s) 2024   OPEN

Abstract

The non-destructive stress measurement method is the main trend in residual stress analysis. The ultrasonic method, which utilizes the acoustoelastic effect of the longitudinal critically refracted (LCR) wave, is one of the time-saving measurement techniques. During the practical stress measurement on a workpiece, various external factors may impact the transmission of acoustic waves and the resulting stress value. This study revealed and discussed the effects of four factors on the LCR wave: surface roughness of the examined material, temperature of the material, external mechanical vibration, and surface paint. The stress coefficient was determined by comparing the offset time of the acoustic wave with the stress measured by X-ray analyzer in the zero-stress specimens, which had undergone annealing and deep cryogenic treatment. The test results indicated that the surface roughness did not affect the transition time of the acoustic wave, but it did decrease the intensity of the signal. The increase in temperature and the transition time of the acoustic wave were in a linear relationship. Mechanical vibrations from the environment would not affect the transition time or signal intensity of the acoustic wave, whereas the application of surface paint increased the transition time. Although the effect of paint on the actual workpiece could not be easily modified during stress measurement, the ultrasonic method was still suitable for monitoring the stress of a specific position of the workpiece throughout its operational lifetime. The experiment data in this study were applied to measuring the residual stress of an aluminum ship component, and the result showed a good correspondence with X-ray stress analyzer results.

Highlights

- The surface roughness of tested workpiece does not affect the LCR measured residual stress.
- The linear relationship of LCR signal and temperature can be applied for revising the measured stress value.
- The external mechanical vibration does not influent the LCR wave signal or measured stress.

✉ Weite Wu, wwu@dragon.nchu.edu.tw; Hsuan-Han Lai, jack210810@hotmail.com; Deng-Han Yan, ydh996@gmail.com; Wei-Jheng Chang, cwj@soic.org.tw; Kun-Hsien Chung, khchung@soic.org.tw; Li-Xue Xing, xing493@soic.org.tw; Wei-Ting Chang, f14001224@soic.org.tw | [1]Department of Materials Science and Engineering, National Chung Hsing University, 145 Xingda Road, South Dist., Taichung City 402202, Taiwan, R.O.C.. [2]Ship and Ocean Industries R&D Center, 14F, No.27, Sect. 2, Zhongzheng E. Road, Tamshui Dist., New Taipei City 251401, Taiwan, R.O.C..

Discover

1 Introduction

The residual stress has significant effects on the fatigue life, distortion, dimensional stability, and corrosion resistance of materials or structural components [1, 2]. It is essential to characterize the residual stress in order to evaluate the service reliability of a workpiece. Various techniques and methods, categorized into destructive and non-destructive types, have been developed to measure the residual stress in structures [3]. Destructive methods such as hole-drilling, ring-core, and contour methods were seldom applied due to their destructive and irreversible nature. Non-destructive methods were more favored in practical stress analysis. The X-ray diffraction method was the most widely applied non-destructive stress analysis technique [4]. It was able to examine almost all commercial metals and alloys, such as steel, copper, aluminum, titanium, nickel, and cobalt. A specialized X-ray stress analyzer has been developed for decades. There were two different calculation models: $\sin^2\psi$ and $\cos\alpha$, both of which were utilized in numerous research studies and examinations [5–7]. The critical limitation of the X-ray diffraction method was the depth, which was a few micrometers for steels and tens of micrometers for aluminum alloys [8]. If the tested sample was ground or scratched before diffraction, the measured stress belonged to the deformed layer instead of the true stress of the sample itself. Therefore, additional surface treatment, such as electropolishing, was necessary before conducting diffraction [9]. Another disadvantage of the X-ray diffraction method is that the diffraction signal is not ideal when the tested material has coarse grains or texture. It is preferred to have relatively fine and random grains [10].

The ultrasonic method is another non-destructive technique. Ultrasonic stress measurement techniques are based on the relationship between the speed of acoustic waves and stress. This acoustic wave is generated by an ultrasonic transducer, and the wave patterns can be longitudinal or shear waves; both are reported to be able to evaluate stress [11]. Among the various wave patterns, a particular longitudinal wave exhibits the highest sensitivity to stress [12]. This longitudinal wave refracted at the material's surface upon entering the material and propagated through the material surface. Therefore, the wave is also called a Longitudinal Critical Refracted (LCR) wave, and the stress measurement method is referred to as the LCR method. The quantification of stress relied on a linear relationship between stress (within the elastic limit) and the change in acoustic LCR wave transmission time, also known as the acoustoelastic effect [13]. The greatest advantage of the LCR method is that it is not limited to measuring metals and alloys; it can also be applied to polymers [14] and ceramics [15]. To perform ultrasonic stress measurements on a material, it is necessary to have the acoustoelastic constant (also known as the stress constant) of the tested material for calculation [15, 16]. For different materials and various ultrasonic devices, the stress constant would be unique. The process of determining the stress constant of various materials can be lengthy and time-consuming. The outstanding advantage of the ultrasonic method is its short measurement time, which is a few seconds, compared to the few minutes required by X-ray instruments.

Some factors that affect the transmission of acoustic waves have been discussed, including material anisotropy [17], microstructure and texture [18], and environmental temperature [19]. The impact of anisotropy on acoustic wave speed may not be readily apparent, and the measurement error is minimal and deemed acceptable [17, 20], unless there is a clear or distinct structural alteration [21]. Consequently, the influence of anisotropy should not pose a challenge during practical measurements. The effect of temperature, including the surrounding environment and the tested material itself, would be more significant [17, 19, 22]. This involves a linear relationship between the temperature and the acoustic transition time, which could still be modified. For practical ultrasonic applications on workpieces or structures, there are other factors that affect the acoustic transmission. For example, the surface roughness of the material affects acoustic wave reflections and scattering [24], but its impact on transition time has not been reported yet. The effect of environmental external vibrations on the acoustic transition time has not been discussed. The paint on the material may affect the acoustic properties, but it is still be tolerable for ultrasonic inspection [25]. However, this may not hold true for stress measurement. As mentioned above, these factors still require discussion. Therefore, the aim of this study was to investigate how environmental factors such as surface roughness, external mechanical vibration, and surface paint affect acoustic transmission during stress measurement using the LCR method.

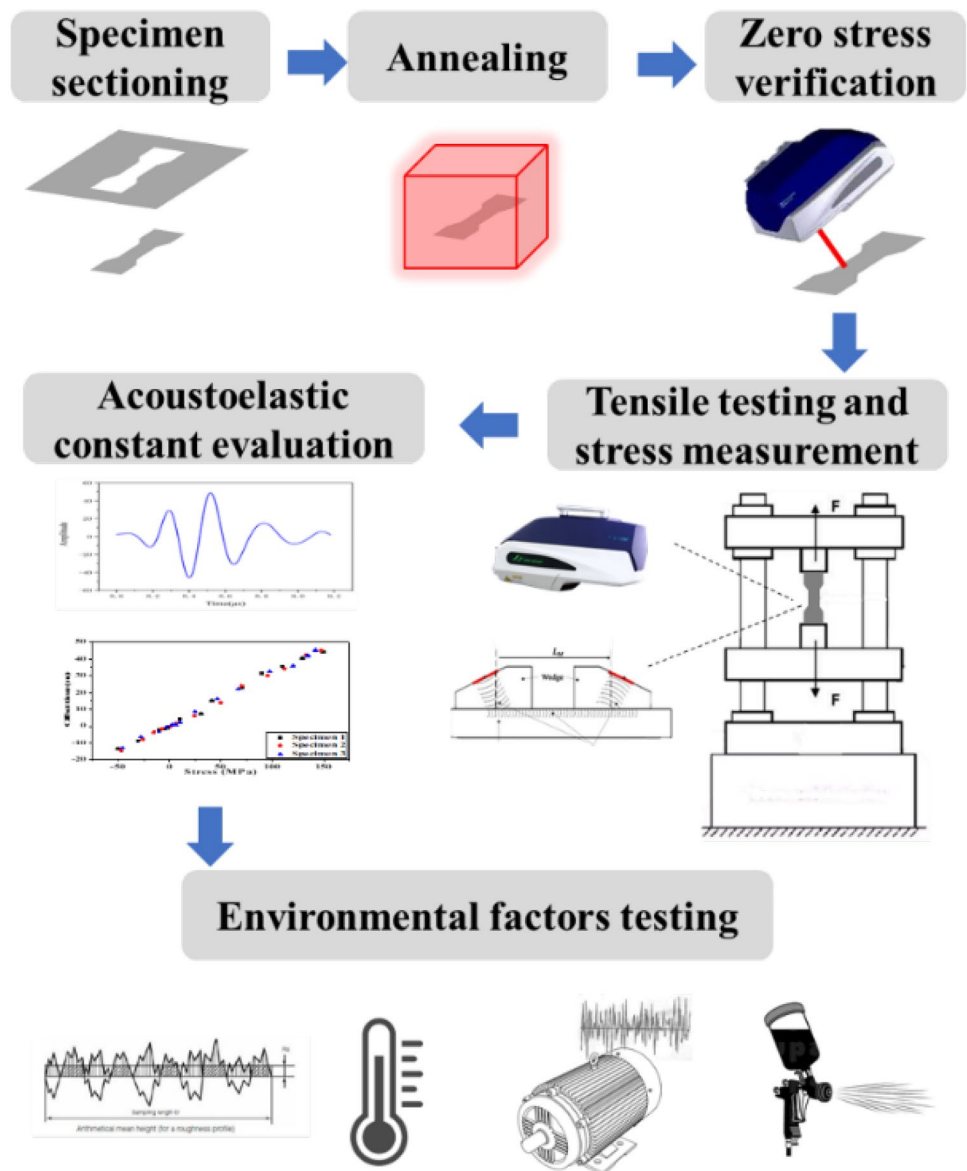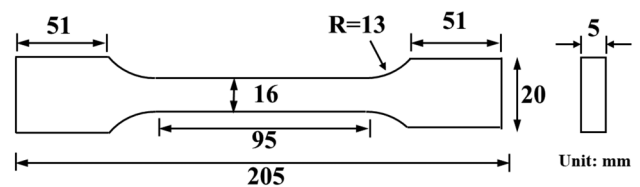**Fig. 1** The experimental procedure illustration

Fig. 2 Illustration of ultrasonic probe

2 Experiments

The experimental procedure is illustrated in Fig. 1. The raw material used in this study was AA5083-H116 plates with a thickness of 4 mm and a composition of 4.57% Mg–0.74% Mn–0.3% Fe and balanced Al, all in weight percent. The as received aluminum plates were cut into the shape of tensile test specimens according to the ASTM B557M-15 standard [26]. The specimen dimensions are illustrated in Fig. 2. The sectioned specimens were annealed at 250 °C for 30 min and then cooled down to room temperature at a rate of 1 °C/min in order to release the residual stress before testing. The annealing temperature of 250 °C was chosen to reduce the susceptibility of the alloy to intergranular

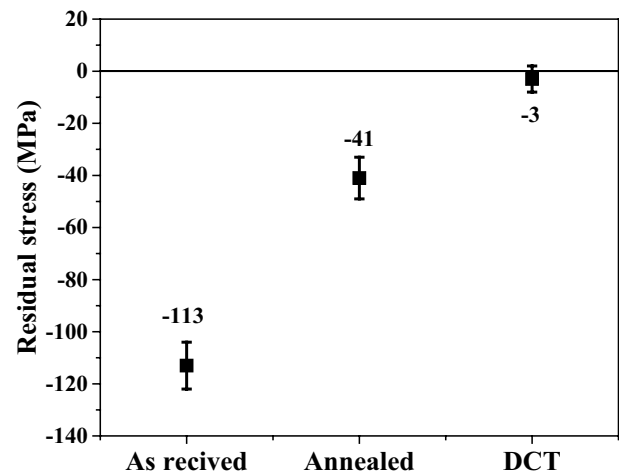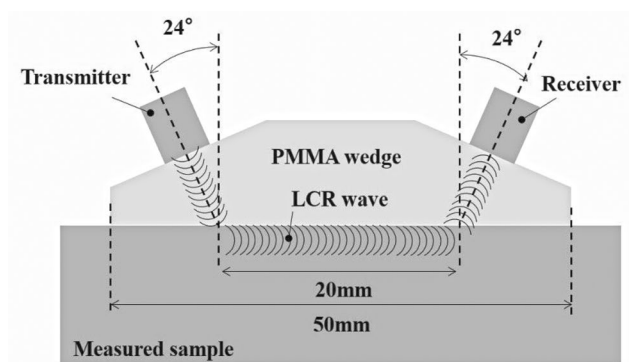**Fig. 3** The residual stress of specimens after different treatment

Fig. 4 Illustration of ultrasonic probe

corrosion, and the microstructure remained relatively unchanged after annealing [27]. After annealing, the residual stress of the specimen was measured to confirm that it had reached a state of zero-stress.

After annealing, the residual stress and the acoustic wave transmission time were measured to assess the specimens' initial condition. The X-ray diffraction method was used to quantify stress, and the stress was calculated using the cosα model, which had been utilized in a previous study [28]. A Pulstec μ-X360s X-ray stress analyzer was utilized in this study. The incident beam was Cr–Kα radiation with the tube voltage of 30 kV, the tube current of 1 mA, a wavelength of 2.29 Å, and the incident angle was 30° from the normal direction of the specimen surface. Stress analysis was conducted by measuring the {311} lattice plane of the α-Al phase at a Bragg angle of 139° and collect the diffraction Debye-ring. The other calculation constants included the Young's modulus 68.9 GPa, the Poisson's ratio 0.33. Theoretically, the residual stress should be close to zero after annealing. However, in practice, most of the specimens exhibited compressive stress levels ranging from −50 to −40 MPa. To eliminate this compressive stress, the annealed specimens underwent the deep cryogenic treatment (DCT) which was reported to reduce the residual stress of different aluminums [29–31]. In this study, the deep cryogenic treatment process was to immerse the specimens in a tank filled with liquid nitrogen for 24 h. Figure 3 shows the measured residual stress of as received, annealed and after DCT specimens. The true zero-stress specimens were obtained after DCT.

The transmission time of acoustic waves was measured using the Jianwei Technology USG ultrasonic stress analyzer. A probe with a 24° acoustic incident angle and a fixed distance of 20 mm between the transmitter and receiver, which were both embedded in a PMMA wedge and the transmitter emitted a 5 MHz frequency acoustic wave, as shown in Fig. 4. Carboxymethyl cellulose (CMC) was uniformly applied to the specimen surface as a coupling agent during measurement. The acoustic waveform and transmission time of the zero-stress specimen were identified as the reference, as shown in Fig. 5. The first peak of the received signal was at 8.18 μs, and both the room and specimen temperature were 25 ± 2 °C. Once the zero-stress and transmission time were identified, tensile testing was conducted on the specimens. As a fixed tensile load was applied to a specimen, its residual stress and acoustic wave transmission time were both measured. The stress was measured

Fig. 5 The acoustic signal and the LCR wave measured from the zero-stress specimen
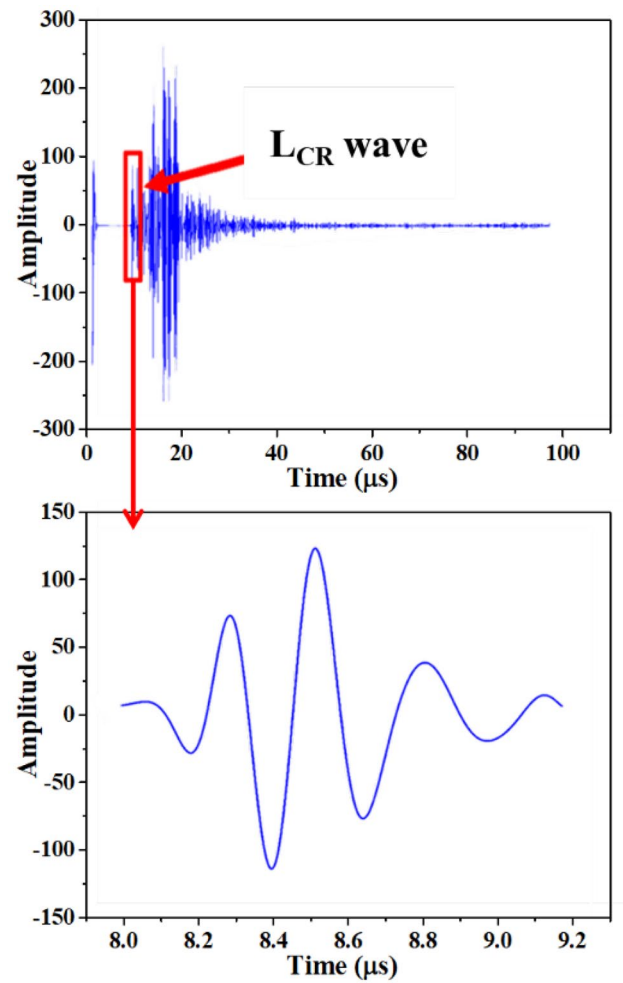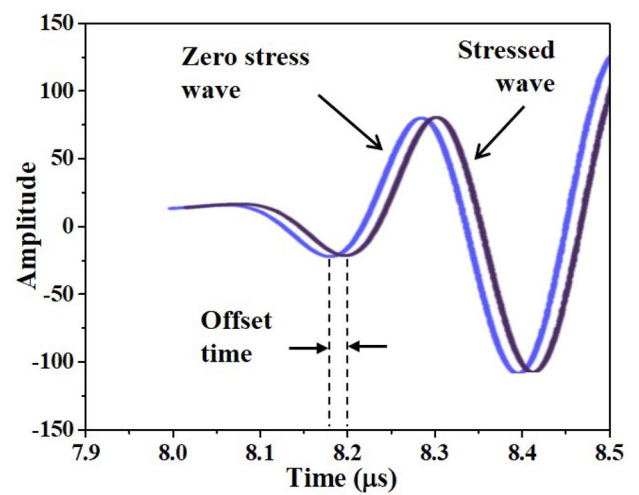

Fig. 6 The offset time versus specimen stress

using an X-ray instrument to determine the actual stress of the specimen. The yield stress of AA5083-H116 is 200–220 MPa. For this study, the maximum tensile stress applied to the specimen was 150 MPa. The offset time was calculated from the measured acoustic wave and the zero-stress wave as shown in Fig. 6. The acoustoelastic constant (stress constant) K could be calculated from the offset time using the equation derived by Xu [15]:

$$\Delta\sigma = K \times \Delta t, \tag{1}$$

where $\Delta\sigma$ was equal to measured stress and Δt was the offset time, since the zero-stress specimen and its acoustic transmission time had been identified.

Four environmental factors were selected for discussion regarding their impact on LCR measurement: sample surface roughness, temperature, mechanical vibration, and the presence of paint on the sample surface. After verifying the stress constant, the four factors were applied to the specimens, and the effect on the acoustic wave was analyzed and discussed individually.

3 Determination of the stress coefficient and verifying

Figure 7 displays the residual stress of the specimen, as measured by the X-ray stress analyzer, along with the corresponding acoustic wave offset time. As mentioned, the annealed specimens exhibited compressive stress. Some annealed specimens that did not undergo DCT were subjected to the loading test; consequently, compressive stresses were recorded in Fig. 7. When the specimens with compressive stress were tested, the acoustic wave appeared on the left side of the zero-stress wave, resulting in a negative offset time change. The tensile testing was conducted when both the room and specimen temperatures were 25 ± 2 °C. As the tensile force applied to the specimen increases gradually, the measured stress transitions gradually from compression to tension, allowing for the measurement of the offset time of LCR wave transmission. An obvious linear relationship could be fitted to the curve. The slope of the fitted curve was 3.23 MPa/ns, representing the stress constant K of AA5083-H116 aluminum in this study. It should be noted that this stress constant was only used in this study. For the same tested material with different instruments and test conditions, the stress constant would not be consistent. For example, Guo reported that the stress constant of 5083 ranged from 5.09 to 6.71 MPa/ns, depending on the location of the weld metal [16]. Furthermore, while the LCR technique was found to be more sensitive to stress and less sensitive to microstructure or texture [32], it is important to note that significant structural changes still influenced the acoustoelastic constant [21, 33]. A common example is the variation in stress constants reported for the weld metal, heat-affected zone, and base metal [16, 34]. The specified stress constant in this study is only applicable with the identical ultrasonic instrument and AA5083-H116 plate.

To validate the calculated stress constant, a second tensile test was conducted. The tested sample was the zero-stress specimen, and both the X-ray stress analyzer and ultrasonic stress analyzer were used to analyze the sample under loading conditions. Figure 8 presents the loading stress measured by the X-ray stress analyzer and the stress

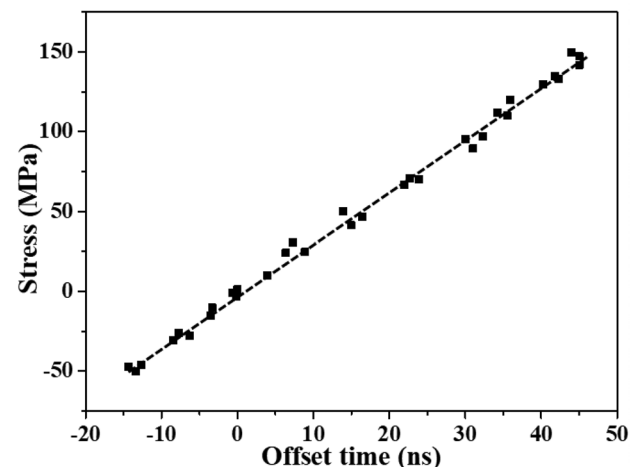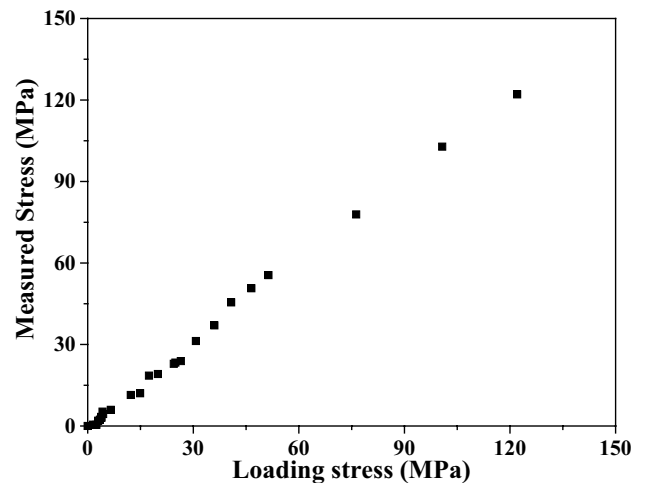**Fig. 7** The offset time versus specimen stress

**Fig. 8** Loading stress and corresponding LCR measured stress during tensile test

measured by the ultrasonic stress analyzer using the stress constant K = 3.23 MPa/ns. The two measured results showed good agreement. The stress measured by the LCR was sensitive to the applied load. In addition, the operation time of the ultrasonic stress analyzer was only tens of seconds, which was advantageous compared to the X-ray stress analyzer that required a few minutes to complete a test.

4 Testing with different environmental factors

4.1 Surface roughness

For regular ultrasonic defect inspection, surface roughness led to strong signal noise [35, 36], making it difficult to identify the signal of cracks [37]. Therefore, in the research on LCR versus residual stress, the tested specimens were mechanically ground or machined to eliminate the effect of surface roughness [38, 39]. However, the surface of a workpiece may not be flat or polished. Grinding scratches or marks are common on a metal surface. The impact of surface roughness on the transition of LCR has not been reported yet. To compare the impact of surface roughness on acoustic waves, the test specimens were ground using abrasive sandpaper of different grit sizes. To maintain the specimens in a zero-stress state, manual grinding was performed with gentle pressure and in a random direction. The surface roughness was measured using a Mitutoyo SJ-210 roughness meter. The zero-stress specimen had a surface roughness of Ra 1.2 μm. After grinding,

Fig. 9 The LCR wave of specimens with different surface roughness
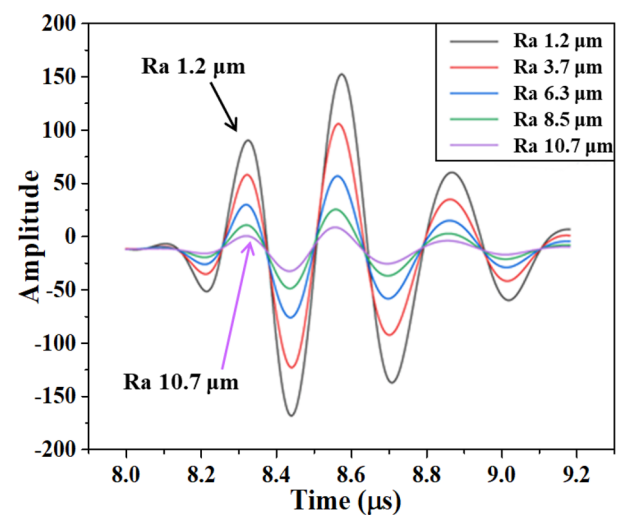
the specimens had roughness values of Ra 1.2 μm, 3.7 μm, 6.3 μm, 8.5 μm, and 10.7 μm for testing. The acoustic waveforms of various specimens are depicted in Fig. 9. Five different LCR waveforms exhibited significant differences in amplitude. The specimen with the highest roughness (Ra 10.7 μm) had the lowest wave amplitude, while the one with the lowest roughness (Ra 1.2 μm) had the highest wave amplitude. It was believed that the ultrasonic wave exhibited multiple reflections and was absorbed by microcavities when propagating through the rough surface [24]. When the test sample had a lower surface roughness, the ultrasonic probe could establish better contact with the measured area. This resulted in more efficient transmission of ultrasonic energy into the workpiece and reduced scattering. Conversely, as the roughness increased, more ultrasonic energy was scattered, leading to a decrease in the received wave signal. Luo reported that there was an exponential relationship between surface roughness and wave amplitude [40]. The author proposed a method to modify this effect which necessitated additional signal processing. Apart from the waveform of Ra 1.2 μm, a slight leftward shift is noticeable in the other waveforms. The reason for this is the surface compressive stress induced during grinding, which was not intense enough to cause a significant shift in the waveform. The surface roughness did not significantly affect the location of LCR waveform peaks. During testing, compression took place at the surface of the specimen after grinding, while the inner material remained under zero stress. Considering that the measured depth was approximately 1 mm below the surface using a 5 MHz frequency [21], minor surface grinding stress would not impact the measured result. In conclusion, when applying the LCR method for stress measurement to a workpiece, slight surface grinding would enhance the reception of a clearer acoustic signal and would not necessitate additional signal processing. This restriction would be advantageous because surface grinding is prohibited when employing the X-ray method. In this study, the LCR waves were identifiable when the surface roughness was lower than Ra 10.7 μm. Therefore, one can consider the roughness Ra 10 μm as the maximum tolerance, as suggested in Xu's report [15].

4.2 Temperature

The temperature of a metal affects the acoustic velocity (or speed of sound). As the metal temperature increased, the acoustic velocity decreased; similar results were found in studies of steels [41] and aluminum [42]. When measuring the stress of a metal using the LCR method, variations in the metal's temperature can result in measurement errors, as the environmental temperature may not always be 25 °C. Interestingly, the acoustic velocity change versus temperature for the ultrasonic wave exhibited a linear relationship [43, 44]. The linear relationship could be used to adjust the measured result and eliminate the temperature effect.

To investigate the impact of specimen temperature on the LCR wave, an ultrasonic probe was used to measure the zero-stress specimen heated to various temperatures. The specimen was heated using a hot plate, and the temperature was measured with a ONEWAY OWI-400 infrared thermometer. The maximum testing temperature was 65 °C. The LCR wave at different specimen temperatures and the offset time of different temperatures compared to the basic wave (at 25 °C), were both recorded and illustrated in Fig. 10. In Fig. 10a, the wave of the heated specimen shifted to the right, indicating a reduction in wave speed and an increase in the time required for transmission. The
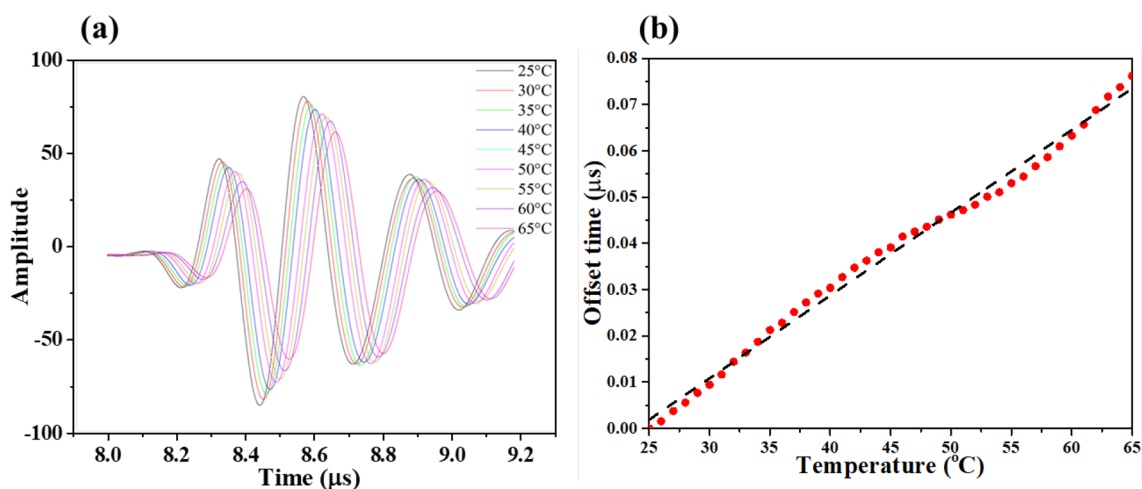

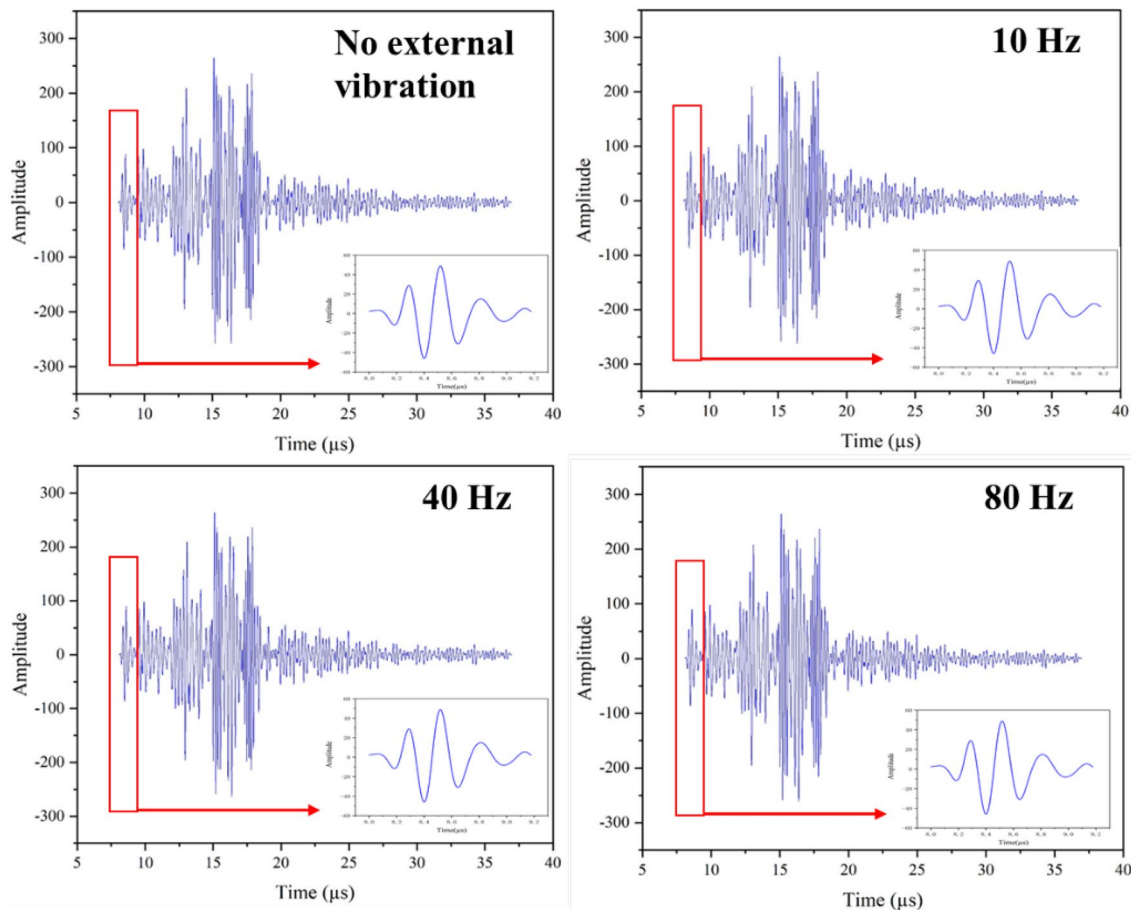**Fig. 10** The **a** LCR wave and **b** offset time versus specimen temperature

Fig. 11 The acoustic waves under different external vibration frequency

higher the temperature of the specimen, the longer the wave transmission time and the offset time, as illustrated in Fig. 10b. The relationship between offset time and temperature could be modeled with a linear curve, which had a slope of 1.79 ns/°C. As mentioned, the stress constant K of 5083-H116 in this study was 3.23 MPa/ns. Through a simple multiplication, the influence of temperature was calculated to be 5.78 MPa/°C. Temperature fluctuations may lead to significant measurement errors. For example, if a metallic structure is placed outdoors and exposed to direct sunlight, its temperature could rise to over 45 °C, resulting in a temperature deviation of 20 °C and a measurement error of 115.6 MPa. A similar result was shown in Fraga's report [22], which found that the temperature impact for steel was 15.9 ns/°C for acoustic transmission time and 64 MPa/°C for measured stress deviation. Fraga concluded that this could be attributed to the PMMA base of the probe and the properties of the tested material. Zeng's study showed that the temperature impact on the ultrasonic wave transmission was not only in the tested metal but also in PMMA wedge [45], and the author suggested to correct the thermal effect on the PMMA wedge. Fraga's research suggested reducing the wave travel path in the tested material to minimize the impact of temperature. However, this would require a higher data acquisition rate to uphold signal quality. Reducing the wave path in PMMA wedge could be the alteration. One could also notice that the temperature influence on transmission time was 1.79 ns/°C in this study (AA5083 aluminum), while that was 15.9 ns/°C for steel in the reference. In the report on AA7050 aluminum by Wang et al., the temperature impact was 3.25ns/°C [23], whereas it was – 19.8 ns/°C in Liu's study [24]. Although Liu did not explain why the constant was negative, it could still be considered that the temperature impact would not be the same with different ultrasonic instruments, even though the tested materials were similar. In practical measurement operations, linear calculation could be applied to the LCR instrument to eliminate the effects of

Fig. 12 The LCR waves of un-painted and painted specimens
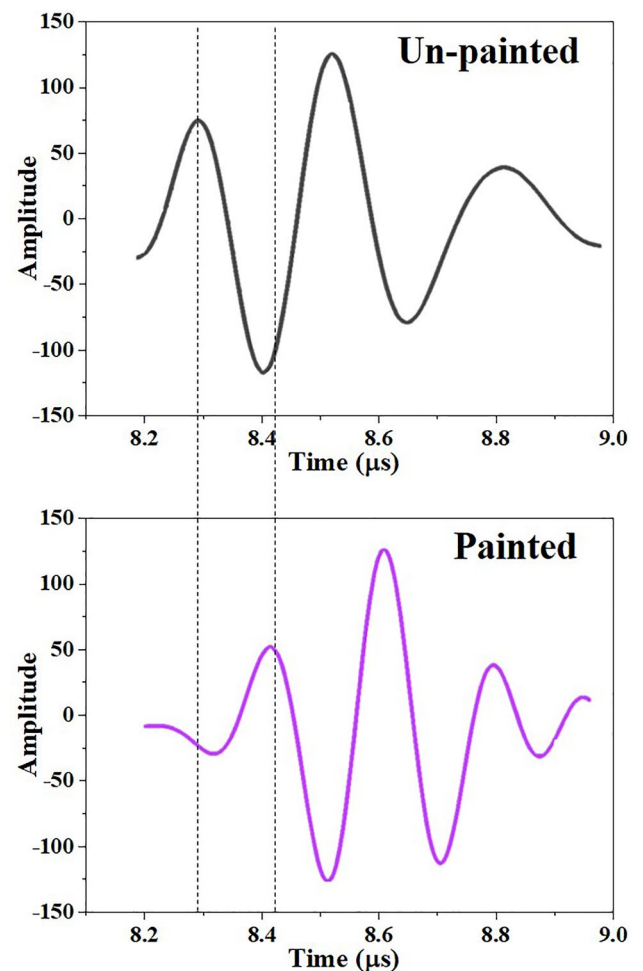
4.3 Mechanical vibration

The external vibration caused by the engine, generator, or motor may be unavoidable during the measurement operation of a practical workpiece. One might think that external vibrations could affect the transmission of acoustic waves; however, there has been no research on this topic. To investigate the impact of vibration frequencies on the LCR wave transit time, we applied various frequencies to the zero-stress specimen during ultrasonic measurements. The external vibration source was an eccentric rotating motor with a maximum acceleration of 2G. Both the specimen and the motor were secured to a table. The mechanical vibration frequency ranged from 10 to 80 Hz. The LCR waves measured at various vibration frequencies are depicted in Fig. 11. The results showed that all external vibrations with different frequencies did not affect the LCR wave or any other acoustic waves. This result has not been reported or discussed yet. The acoustic wave signal only changes when there is a source that involves a change in the wave phase, such as a modification in wave path length and wave speed. This is the fundamental function of an ultrasonic receiver [46]. The external vibration
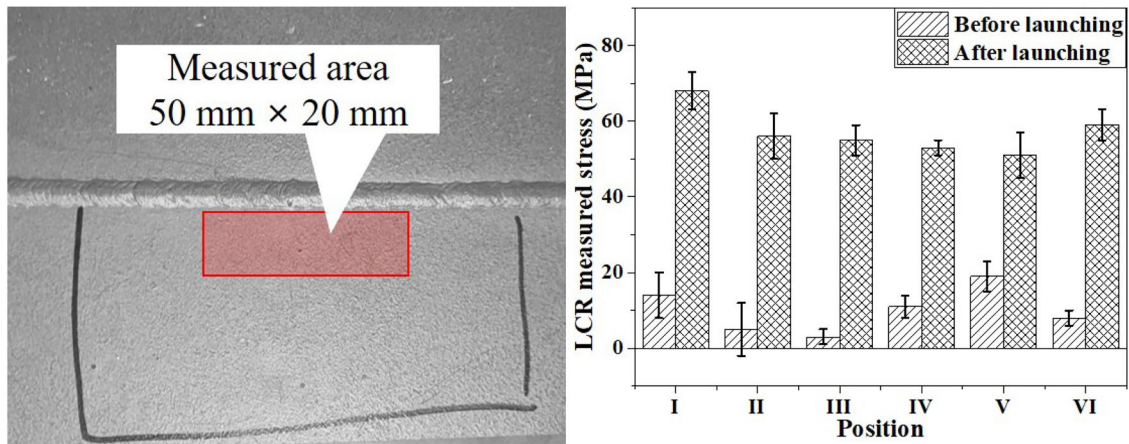
Fig. 13 The application of LCR method to examine a painted aluminum plate of a ship

did not affect the phase of the acoustic wave, so the received LCR signal remained constant despite the varying external vibrations. Preliminary evaluation indicated that the external vibration would not affect the LCR waves. Now, there is one more advantage of the LCR method. During the LCR stress measurement process, the operator does not have to worry about the measured results being influenced by the vibration of the structure being measured.

4.4 Surface paint

Protective coatings are applied to specific metal components to prevent surface corrosion. One of the most effective methods is painting because of its affordability, ease of application, and low maintenance requirements. For regular ultrasonic inspection, the presence of paint may still be tolerable, although it may affect the acoustic properties [25, 47, 48]. The impact of paint on wave transmission time still needs to be discussed in relation to stress measurement using the LCR method. Therefore, a zero-stress sample was used for measurement in this experiment. The paint was manufactured by Yung Chi Paint Corp., and it was type No. 1020, an epoxy alloy primer. The zero-stress specimen was painted at room temperature. After the paint had dried, the thickness of the coated paint was examined to be approximately 0.25 mm, and the subsequent LCR measurement was performed. Figure 12 shows the LCR waveforms of specimens with and without surface paint. The acoustic transit time in the painted specimen increased by 0.13 μs, and the wave

Fig. 14 The aluminum ship structure, its weld seam and raw material plate for LCR test
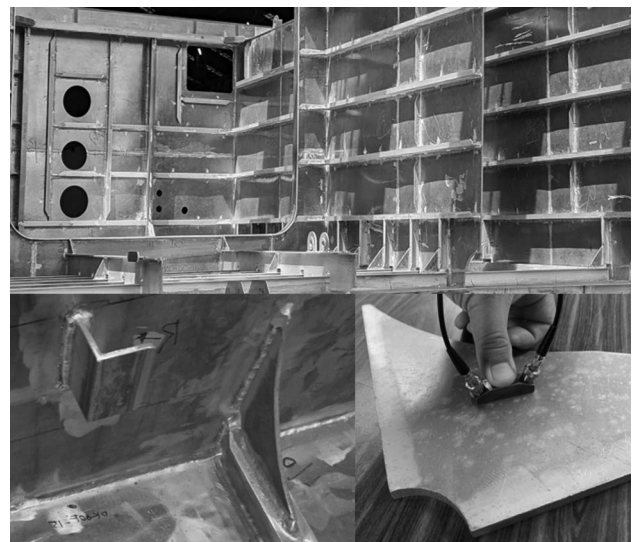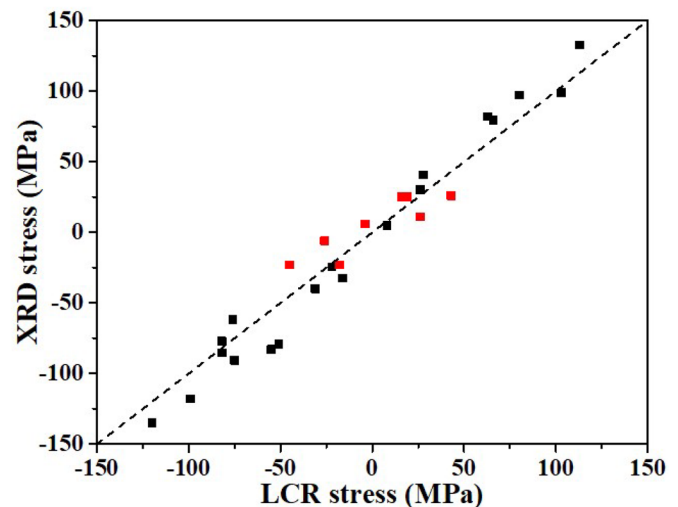
Fig. 15 The LCR and X-ray measured (XRD) stress of the components in Fig. 14

amplitude of the painted specimen decreased slightly. Basically, the speed of sound in aluminum (over 6000 m/s [49]) is faster than in epoxy-based material (about 1000 m/s [50]); therefore, the received waveform in Fig. 12 should travel through the aluminum surface, not through the paint layer. By simply multiplying the stress constant of 3.23 MPa/ns, the measured stress value of the zero-stress specimen increased by 420 MPa. The increase in acoustic transit time was predictable because the acoustic wave must refract twice as it passes through the boundary between the paint layer and the metal. Furthermore, some waves leaked into the paint layer, resulting in a decrease in wave amplitude [51]. In practical applications, the type of paint material and its thickness may vary depending on the specific environment or intended purpose. Therefore, correcting the measured stress value based on the transit time increase would not be an effective solution. However, the LCR method was still suitable for monitoring stress at a fixed location on the painted metal workpiece. For example, the application of the LCR method to monitor the stress of an aluminum ship welding is shown in Fig. 13. The results showed that the tensile welding stress of the aluminum ship increased after its launch. One could continue to monitor the residual stress of this ship's frame or shell after prolonged navigation.

4.5 Application of LCR measurement on a ship structure

To verify and test the LCR constant and calculation from the above experiments, LCR measurements were conducted on a ship component made of AA5083 aluminum, as shown in Fig. 14. The measured positions included those located near the weld seam of the component and those of unwelded plates. The measured positions included those located near the weld seam and those of unwelded plates. Some components were exposed to sunlight, with temperatures ranging from 40 to 50 °C. The measurements from these areas were adjusted to account for temperature variations. An X-ray stress analyzer was also used to measure the same positions. Both the stresses analyzed by LCR and X-ray were plotted in Fig. 15, where the red points were temperature-corrected. Although there were still discrepancies between stresses measured by LCR and X-ray, the ultrasonic LCR method remained a suitable measurement for practical components. The measured stress deviation should come from the X-ray because the surface condition of the component (mainly the roughness and oxidation layer) might affect the calculated stress, while the LCR wave could overcome these limitations. As mentioned, the LCR method was suitable to monitor the residual stress of the ship component or structure.

5 Conclusions

The study conducted the ultrasonic stress measurement method on AA5083-H116 aluminum, analyzing the longitudinal critically refracted (LCR) wave transmission time offset. The acoustoelastic constant used in this study was 3.23 MPa/ns. The influence of four different environmental factors on LCR wave transmission was examined, and the following conclusions could be drawn.

a) The higher surface roughness of the tested sample would not affect the wave transmission offset time, but it would result in a lower amplitude of the received wave signal. For practical measuring operations, slight surface grinding would help in receiving a better acoustic signal and could still measure the residual stress within the material.

b) As the sample temperature increased, the wave transmission time also increased. The time offset was found to be correlated with the temperature in a linear relationship, with a slope of 5.78 MPa/°C.

c) Mechanical vibrations from the surroundings did not alter the LCR wave or transmission time; therefore, they would not affect the measurement operation when applying to the workpiece.

d) The surface paint clearly caused an increase in the wave transmission time. For practical measurement of the painted workpiece, the LCR method is not suitable for stress measurement, but it is appropriate for stress monitoring of a fixed location of the workpiece or structure.

Data availability The datasets generated and analyzed during the current study are available from the corresponding author on reasonable request.

Declarations

Competing interests The authors declare that they have no known competing financial interests or personal relationships that could have appeared to influence the work reported in this paper.

References

1. Gou G, Zhang M, Chen H, Chen J, Li P, Yang YP. Effect of humidity on porosity, microstructure, and fatigue strength of A7N01S-T5 aluminum alloy welded joints in high-speed trains. Mater Design. 2015;85:309–17.
2. Totten GE, Howes M, Inoue T. Handbook of residual stress and deformation of steel. Materials Park: ASM International Publishers; 2002. p. 417–44.
3. Rossini NS, Dassisti M, Benyounis KY, Olabi AG. Methods of measuring residual stresses in components. Mater Design. 2012;35:572–88.
4. Shao Z, Zhang C, Li Y, Shen H, Zhang D, Yu X, Zhang Y. A review of non-destructive evaluation (NDE) techniques for residual stress profiling of metallic components in aircraft engines. Aerospace. 2022;9:534.
5. Delbergue D, Texier D, Levesque M, Bocher P. Comparison of two X-ray residual stress measurement methods: $sin^2\psi$ and $cos\alpha$, through the determination of a martensitic steel X-ray elastic constant. Mater Res Proc. 2016;2:55–60.
6. Li Z, Xue B, Cui Y, Zhou G, Zhang S, Lu N, Wen L, Zhang D. NDT of residual stress in thick aluminum alloy plates under different aging conditions using multiple techniques. Materials. 2016;15:8732.
7. Lai HH, Wu W. Practical examination of the welding residual stress in view of low-carbon steel welds. J Mater Res Technol. 2020;9:2717–26.
8. Valentini E, Beghini M, Bertini L, Santus C, Benedetti M. Procedure to perform a validated incremental hole drilling measurement: application to shot peening residual stresses. Strain. 2011;4:e605–18.
9. ASTM E2860-12. Standard test method for residual stress measurement by X-ray diffraction for bearing steels. ASTM International; 2012.
10. Meisner L, Lotkov A, Ostapenko M, Gudimova EY. X-ray diffraction study of residual elastic stress and microstructure of near-surface layers in nickel-titanium alloy irradiated with low-energy high-current electron beams. Appl Surf Sci. 2013;280:398–404.
11. Li Z, He J, Teng J, Huang Q, Wang Y. Absolute stress measurement of structural steel members with ultrasonic shear-wave spectral analysis method. Struct Health Monit. 2019;18:216–31.

12. dos Santos AA Jr., Bray DE. Comparison of acoustoelastic methods to evaluate stresses in steel plates and bars. J Press Vessel Technol ASME. 2002;124:354–8.
13. Bray DE, Stanley RK. Nondestructive evaluation: a tool in design. Boca Raton: CRC Press; 1997.
14. Jia D, Bourse G, Chaki S, Lacrampe MF, Robin C, Demouveau H. Investigation of stress and temperature effect on the longitudinal ultrasonic waves in polymers. Res Nondestruct Eval. 2014;25:20–9.
15. Xu C, Song W, Pan Q, Li H, Liu S. Nondestructive testing residual stress using ultrasonic critical refracted longitudinal wave. Phys Procedia. 2015;70:594–8.
16. Guo M, Gou G, Chen B, Qiu F, Zhu Z, Jin J, Wu X, Gao W, Sun S. Ultrasonic correction measurement for residual stress in 5083 aluminum alloy welded component of high-speed train. Metals. 2023;13:137.
17. Augereau F, Laux D, Allais L, Mottot M, Caes C. Ultrasonic measurement of anisotropy and temperature dependence of elastic parameters by a dry coupling method applied to a 6061-T6 alloy. Ultrasonics. 2007;46:34–41.
18. Kube CM, Arguelles AP, Turner JA. Ultrasonic backscatter from elongated grains using. Ultrasonics. 2018;82:79–83.
19. Zou D, Liu T, Liang C, Huang Y, Zhang F, Du C. An experimental investigation on the health monitoring of concrete structures using piezo-electric transducers at various environmental temperatures. J Intell Mater Syst Struct. 2015;26:1028–34.
20. Li Y, Liu H, Liu Y, Zhang X, Wang Y. In-plane elastic anisotropic constants (IEACs) measurement of rolling aluminum plate at different depth using ultrasonic LCR wave. Appl Acoust. 2019;149:59–67.
21. Javadi Y, Hloch S. Employing the L_{CR} waves to measure longitudinal residual stresses in different depths of a stainless steel welded plate. Adv Mater Sci Eng. 2013;2013: 746187.
22. Fraga RS, Santos AA, Andrino MH. Temperature effect on the measurement of stresses in pipelines using ultrasonic L_{cr} waves. In: Proceedings of the ASME 2008 international mechanical engineering congress and exposition. Boston, Massachusetts, USA; 2008. p. 361–7.
23. Wang X, Shi Y, Liang J, He F, Tao C. Stress in pre-stretched aluminum alloy plate by acoustic elasticity. J Mater Eng. 2015;43:95–100.
24. Liu H, Li Y, Li T, Zhang X, Liu Y, Liu K, Wang Y. Influence factors analysis and accuracy improvement for stress measurement using ultrasonic longitudinal critically refracted (LCR) wave. Appl Acoust. 2018;141:178–87.
25. Santo J. Use of industrial ultrasound for welded joints on painted surfaces with naval industry applications. In: International ultrasonic testing online conference, e-journal of nondestructive testing. 2021;26.
26. ASTM B557M-15. Standard test methods for tension testing wrought and cast aluminum-and magnesium-alloy products. ASTM International; 2015.
27. Yen CH, Wu CT, Chen YH, Lee SL. Effects of annealing temperature on stress corrosion susceptibility of AA5083-H15 alloys. J Mater Res. 2016;31:1163–70.
28. Wang JS, Hsieh CC, Lin CM, Chen EC, Kuo CW, Wu W. The effect of residual stress relaxation by the vibratory stress relief technique on the textures of grains in AA 6061 aluminum alloy. Mater Sci Eng A-Struct. 2014;605:98–107.
29. Zhou C, Sun Q, Qian D, Liu J, Sun J, Sun Z. Effect of deep cryogenic treatment on mechanical properties and residual stress of AlSi10Mg alloy fabricated by laser powder bed fusion. J Mater Process Technol. 2022;303: 117543.
30. Zhou J, Xu S, Huang S, Meng X, Sheng J, Zhang H, Li J, Sun Y, Boateng EA. Tensile properties and microstructures of a 2024-T351 aluminum alloy subjected to cryogenic treatment. Metals. 2016;6:279.
31. Araghchi M, Mansouri H, Vafaei R, Guo Y. A novel cryogenic treatment for reduction of residual stresses in 2024 aluminum alloy. Mater Sci Eng A-Struct. 2017;689:48–52.
32. Bray DE, Junghans P. Application of the L_{CR} ultrasonic technique for evaluation of post-weld heat treatment in steel plates. NDT&E Int. 1995;28:235–42.
33. Geľatko M, Hatala M, Vandžura R, Botko F. Longitudinal critically refracted (L_{CR}) ultrasonic wave for residual stress measurement. In: IOP Conf. series: materials science and engineering, Bardejovské Kúpele, Slovak Republic. 2021;1199:012060.
34. Zhu Q, Chen J, Gou G, Chen H, Li P, Gao W. Residual stress measurement and calibration for A7N01 aluminum alloy welded joints by using longitudinal critically refracted (L_{CR}) wave transmission method. J Mater Eng Perform. 2016;25:4181–9.
35. Wang Z, Cheng J. Numerical and analytical study for ultrasonic testing of internal delamination defects considering surface roughness. Ultrasonics. 2021;110: 106290.
36. Hanks E, Palazotto A, Liu D. Effect of surface roughness on ultrasonic inspection of electron beam melting Ti-6Al-4V. J Def Anal Logist. 2019;3:131–41.
37. Wang Z, Cui X, Ma H, Kang Y, Deng Z. Effect of surface roughness on ultrasonic testing of back-surface micro-cracks. Appl Sci. 2018;8:1233.
38. Lu Y, Xu C, Pan Q, Li D. Research on an ultrasonic longitudinal critically refracted wave detection method for the depth distribution of stress. Metals. 2022;12:1602.
39. Yan X, Pang J, Jing Y. Ultrasonic measurement of stress in SLM 316L stainless steel forming parts manufactured using different scanning strategies. Materials. 2019;12:2719.
40. Luo Z, Meng Y, Fan S, Lin L. Assessment of surface/subsurface damage in early-stage fatigue: a new attempt based on LCR wave. Int J Fatigue. 2023;170: 107537.
41. Nowacki K, Kasprzyk W. The sound velocity in an alloy steel at high-temperature conditions. Int J Thermophys. 2010;31:103–12.
42. Singh DP. Ultrasonic studies of aluminium in the temperature range 293 K to 925 K. Indian J Phys. 1990;64A:269–74.
43. Liu Z. Temperature dependence of ultrasonic longitudinal guided wave propagation in long range steel strands. Chin J Mech Eng. 2011;24:487–94.
44. Gonchar A, Mishakin V, Kurashkin K. Thermo-ultrasound method for determining the damage of structural material. MATEC Web Conf. 2018;224:02027.
45. Zeng S, Zhu J, Zhong B, Li X. Thermo-acoustoelastic effect of Rayleigh wave: theory and experimental verification. Ultrasonics. 2023;131: 106948.
46. Singh KM, Sumathi P. Vibration parameter estimation methods for ultrasonic measurement systems—a review. IET Sci Meas Technol. 2015;9:492–504.
47. Whaley HL. Ultrasonic tests on materials with protective coatings. Mater Eval. 1977;35:65–8.
48. Predoi MV, Petre CC. Thin wall pipe ultrasonic inspection through paint coating. Phys Procedia. 2015;70:287–91.

49. Yaghoubi F, Moghanaki SK, Kazeminezhad M. Sound velocity in severely deformed aluminum alloys: AA1100 and AA2024. Appl Phys A-Mater. 2020;126:302.

50. Kagathara VM, Sanariya MR, Parsania PH. Sound velocity and molecular interaction studies on chloro epoxy resins solutions at 30°C. Eur Polym J. 2000;36:2371–4.

51. Fuchs PA, Clark AV, Lozev MG, Halabe U, Klinkhachorn P, Petro S, GangaRao H. Ultrasonic instrumentation for measuring applied stress on bridges. J Nondestruct Eval. 1998;17:141–52.

Publisher's Note Springer Nature remains neutral with regard to jurisdictional claims in published maps and institutional affiliations.